Amphiphilic Treelike Rods at Interfaces: Layered Stems and Circular Aggregation

Jason Holzmueller,[†] Kirsten L. Genson,[†] Yushin Park,[‡] Yong-Sik Yoo,[‡] Myoung-Hwan Park,[‡] Myongsoo Lee,[‡] and Vladimir Tsukruk*,[†]

Materials Science and Engineering, Iowa State University, Ames, Iowa 50011, and Department of Chemistry, Yonsei University, Seoul 120-749, Korea

Received February 15, 2005. In Final Form: April 29, 2005

Amphiphilic dendron−rod molecules with three hydrophilic poly(ethylene oxide) (PEO) branches attached to a hydrophobic octa-*p*-phenylene rod stem were investigated for their ability to form two-dimensional micellar structures on a solid surface. A treelike shape of the molecules was reported to be a major factor in the formation of nonplanar micellar structures in solution and in the bulk state (cylindrical and spherical). We observed that in these treelike amphiphilic molecules the hydrophilic terminated dendron branches assemble themselves in surface monolayers with the formation of two-dimensional layered or circular micellar structures. We suggested the formation of the planar ribbonlike structures with interdigitated layering within the loosely packed monolayers and circular, ringlike structures (2D circular aggregates) in the precollapsed state.

Introduction

Hybrid molecules such as rod−coil molecules and dendritic−linear molecules composed of combined highly branched and linear blocks (dendron−rod, dendron−dendron, dendron−coil) are increasingly investigated, attributable to their unique material properties.[1−4] Asymmetric diblock copolymers such as rod−coil molecules containing a rigid rodlike segment attached to a flexible, coiling segment form novel ordered structures.[5−7] These molecules reorganize themselves from circular aggregates into a regular rectangular lattice in response to changes in surface pressure.[8] Rod−coil molecules form a variety of highly curved micellar structures in solution and in the bulk state. Manipulation of the molecular structure of these hybrid molecules has been shown to result in various solution, bulk, surface, and interfacial structures.[6,9−14] Two-dimensional, zigzag, ribbonlike, helical, and cylindrical structures have been observed for hybrid dendritic−rod and coil−rod molecules by different research groups.[15−20] The overall chemical composition, branching structure, and volume fractions of different blocks dictate the resulting interfacial structures.[21,22] It has been proposed that, by utilizing molecules with complementary and antagonistic structure-forming interactions, systems can be assembled to create order over many length scales.[23] These interactions can originate from very different causes, including hydrophobic and hydrophilic effects,

* Author to whom correspondence should be addressed. E-mail: vladimir@iastate.edu.

[†] Iowa State University.

[‡] Yonsei University.

(1) Bosman, A. W.; Janssen, H. M.; Meijer, E. W. *Chem. Rev.* **1999**, *99*, 1665.

(2) Grayson, S. M.; Frechet, J. M. J. *Chem. Rev.* **2001**, *101*, 3819.

(3) Boas, U.; Heegaard, P. M. H. *Chem. Soc. Rev.* **2004**, *33*, 43.

(4) Zimmerman, S. C.; Zeng, F.; Reichart, D. E. C.; Kolotuchin, S. V. *Science* **1996**, *271*, 1095.

(5) Gopalan, P.; Li, X.; Li, M.; Ober, C. K.; Gonzales, C. P.; Hawker, C. J. *J. Polym. Sci.* **2003**, *41*, 3640.

(6) Lee, M.; Cho, B.-K.; Zin, W.-C. *Chem. Rev.* **2001**, *101*, 3869.

(7) Stupp, S. I.; LeBonheur, V.; Walker, K.; Li, L. S.; Huggins,.K. E.; Keser, M.; Amstutz, A. *Science* **1997**, *276*, 384.

(8) Tsukruk, V.; Genson, K.; Peleshanko, S.; Markutsya, S.; Lee, M.; Yoo, Y.-S. *Langmuir* **2003**, *19*, 495.

(9) Schenning, A. P. H. J.; Elissen-Roman, C.; Weener, J.; Baars, M. W. P. L.; van der Gaast, S. J.; Meijer, E. W. *J. Am. Chem. Soc.* **1998**, *120*, 8199.

(10) Mao, G.; Ober, C. K. *Handb. Liq. Cryst.* **1998**, *3*, 66.

(11) (a) Tsukruk, V. V. *Adv. Mater.* **1998**, *10*, 253. (b) Tsukruk, V. V.; Bliznyuk, V. N. *Prog. Polym. Sci.* **1997**, *22*, 1089. (c) Tsukruk, V. V. *Prog. Polym. Sci.* **1997**, *22*, 247. (d) Luzinov, I.; Minko, S.; Tsukruk, V. V. *Prog. Polym. Sci.* **2004**, *29*, 635.

(12) Frechet, J. M. J. *J. Polym. Sci. Part A: Polym. Chem.* **2003**, *41*, 3713.

(13) Frechet, J. M. J. *Macromol. Symp.* **2003**, *201*, 11.

(14) Tokuhisa, H.; Kubo, T.; Koyama, E.; Hiratani, K.; Kanesato, M. *Adv. Mater.* **2003**, *15*, 1534.

(15) (a) Hawker, C. J.; Bosman, A. W.; Harth, E. *Chem. Rev.* **2001**, *101*, 3661. (b) Mackay, M. E.; Hong, Y.; Jeong, M.; Tande, B. M.; Wagner, N. J.; Hong, S.; Gido, S. P.; Vestberg, R.; Hawker, C. J. *Macromolecules* **2002**, *35*, 8391. (c) Desai, A.; Atkinson, N.; Rivera, F., Jr.; Devonport, W.; Rees, I.; Branz, S. E.; Hawker, C. J. *J. Polym. Sci. Part A: Polym. Chem.* **2000**, *38*, 1033. (d) Marsitzky, D.; Vestberg, R.; Blainey, P.; Tang, B. T.; Hawker, C. J.; Carter, K. R. *J. Am. Chem. Soc.* **2001**, *123*, 6965. (e) Kampf, J. P.; Frank, C. W.; Malmstrom, E. E.; Hawker, C. J. *Polym. Mater. Sci. Eng.* **1999**, *80*, 57.

(16) (a) Chen, J. T.; Thomas, E. L.; Ober, C. K.; Mao, G.-P. *Science* **1996**, *273*, 343. (b) Chen, J. T.; Thomas, E. L.; Ober, C. K.; Hwang, S. S. *Macromolecules* **1995**, *28*, 1688. (c) Gopalan, P.; Zhang, Y.; Li, X.; Wiesner, U.; Ober, C. K. *Macromolecules* **2003**, *36*, 3364.

(17) (a) Mao, G.; Wang, J.; Ober, C. K.; Brehmer, M.; O'Rourke, M. J.; Thomas, E. L. *Chem. Mater.* **1998**, *10*, 1538. (b) Park, J.-W.; Thomas, E. L. *Macromolecules* **2004**, *37*, 3532. (c) Park, J.-W.; Thomas, E. L. *Adv. Mater.* **2003**, *15*, 585. (d) Park, J.-W.; Thomas, E. L. *J. Am. Chem. Soc.* **2002**, *124*, 514.

(18) (a) Li, L.; Beniash, E.; Zubarev, E. R.; Xiang, W.; Rabatic, B. M.; Zhang, G.; Stupp, S. I. *Nat. Mater.* **2003**, *2*, 689. (b) Stendahl, J. C.; Li, L.; Zubarev, E. R.; Chen, Y.-R.; Stupp, S. I. *Adv. Mater.* **2002**, *14*, 1540. (c) de Gans, B. J.; Wiegand, S.; Zubarev, E. R.; Stupp, S. I. *J. Phys. Chem. B* **2002**, *106*, 9730. (d) Zubarev, E. R.; Pralle, M. U.; Sone, E. D.; Stupp, S. I. *Adv. Mater.* **2002**, *14*, 198. (e) Sayar, M.; Stupp, S. I. *Macromolecules* **2001**, *34*, 7135. (f) Sayar, M.; Solis, F. J.; Olvera de la Cruz, M.; Stupp, S. I. *Macromolecules* **2000**, *33*, 7226.

(19) (a) Oh, N.-K.; Zin, W.-C.; Im, J.-H.; Ryu, J.-H.; Lee, M. *Chem. Commun.* **2004**, *9*, 1092. (b) Ryu, J.-H.; Oh, N.-K.; Zin, W.-C.; Lee, M. *J. Am. Chem. Soc.* **2004**, *126*, 3551. (c) Lee, M.; Yoo, Y.-S. *J. Mater. Chem.* **2002**, *12*, 2161.

(20) (a) Percec, V.; Glodde, M.; Bera, T. K.; Miura, Y.; Shiyanovskaya, I.; Singer, K. D.; Balagurusamy, V. S. K.; Heiney, P. A.; Schnells, I.; Rapp, A.; Spiess, H.-W.; Hudson, S. D.; Duan, H. *Nature* **2002**, *419*, 384. (b) Zeng, X.; Ungar, G.; Liu, Y.; Percec, V.; Dulcey, A. E.; Hobbs, J. K. *Nature* **2004**, *428*, 157. (c) Percec, V.; Dulcey, A. E.; Balagurusamy, V. S. K.; Miura, Y.; Smidrkal, J.; Peterca, M.; Nummelin, S.; Edlund, U.; Hudson, S. D.; Heiney, P. A.; Duan, H.; Magonov, S. N.; Vinogradov, S. A. *Nature* **2004**, *430*, 764. (d) Ungar, G.; Liu, Y.; Zeng, X.; Percec, V.; Cho, W.-D. *Science* **2003**, *299*, 1208.

(21) Sendijarevic, I.; McHugh, A. J. *Macromolecules* **2000**, *33*, 590.

(22) Tully, D. C.; Frechet, J. M. J. *Chem. Commun.* **2001**, *14*, 1229.

(23) Muthukumar, M.; Ober, C. K.; Thomas, E. L. *Science* **1997**, *277*, 1225.

10.1021/la0504107 CCC: $30.25
Published on Web 05/27/2005

hydrogen bonding, Coulombic interactions, and van der Waals forces.[24] The self-assembly effects of different constituents on molecular and bulk properties have been observed by utilizing molecules with asymmetric stericity, rigidity, and/or amphiphilic chemisty.[13−35] Minor chemical or conformational changes such as replacing terminal groups of long chains can significant alter the behavior of dendrimer-like molecules under given conditions.[25]

Chemical composition and molecular architecture influence the alignment and packing structure of molecules at interfaces, particularly the air−water interface.[26,27] The molecular fragments are observed to reorganize under applied pressure to the surface of the liquid phase. Amphiphilic molecules orient themselves with the polar constituents being drawn to the water phase while the nonpolar portions of the molecule are repelled by the water phase.[28] This effect can be used to assist with molecular manipulation and self-assembly of molecules into desired structures by balancing amphiphillic and steric factors.[29] As a result, a variety of organized surface structures are formed by nontraditional amphiphiles with branched segments at interfaces.[26,30,31]

Recently, the self-organization of dendron−rod molecules in solution has been investigated.[32−34] Stupp et al. reported the synthesis and self-assembly characteristics of molecules with rodlike, dendritic, and coiled segments.[32] It was predicted that the bulky dendron tail groups would complicate molecular assembly with the linear rod and coil sections. This was found not to be the case, as the molecules were seen to assemble into bimolecular ribbonlike structures with head-to-head packing. Dendron−rod−dendron and dendron−rod molecules with bulky, branched headgroups connected by a rigid chain were synthesized and shown to undergo molecular assembly by Lecommandoux et al.[34] They reported that molecules with a stiff rodlike headgroup and branched dendritic tail groups formed a smectic liquid crystal structure dependent on the rod length. They suggested a strong competition between rod−rod interactions to form a layered structure and packing of the flexible headgroups to create a cubic phase. An asymmetric shape of the molecules was considered to be a major factor in the formation of nonplanar micellar structures in solution and in the bulk state (cylindrical and spherical). However, dense packing of such highly curved, three-dimensional structures would be unfavorable at planar interfaces, and molecular organization under these conditions remains largely unaddressed.

In this study, the properties of "tree shaped" molecules with hydrophilic dendron branches attached to a hydrophobic stem are discerned. These nonsymmetric molecules pair a rodlike hydrophobic fragment with highly branched hydrophilic side chains. The short, flexible poly(ethylene oxide) (PEO) branches were methyl terminated for molecule **1** and hydroxyl terminated for molecule **2** (Figure 1). Similar molecules have been observed to organize into spherical aggregates in solution, but their ability to assemble into organized structures at the air−water interface was not studied.[35,36]

Experimental Section

Three tetrabranched PEO chains were attached asymmetrically to a rigid octa-*p*-phenylene chain at the first and second phenyl rings (Figure 1). The end functionality of the flexible PEO chains was varied from methyl groups (molecule **1**) to hydroxyl groups (molecule **2**). The synthesis for molecule **1** was previously reported and applied to similar molecules.[35,37] Molecule **2** was synthesized according to Scheme 1 and the synthetic procedures described in in the Supporting Information.

Molecular films of these dendritic−rod molecules were fabricated using the Langmuir technique on a RK-1 trough at room temperature (Riegel and Kirstein, GmbH).[38] The trough was located in a laminar flow hood. Compounds were dissolved in chloroform to a concentration of 0.11 mmol/L, and 50 μL of this dilute solution was spread on the water (Nanopure, >18 MΩ cm) subphase. The monolayer was allowed to sit for 30 min to allow the solvent to evaporate. The monolayer was then compressed to the desired surface pressure and deposited on a hydrophilic silicon surface, which was pulled through the layer at a lift speed of 50 μm/s. The deposition of the molecular layer was done according to the standard procedure.[29] Samples were deposited onto polished silicon wafers of the (100) orientation. Wafers were treated in piranha solution (30% hydrogen peroxide, 70% sulfuric acid, *chemical hazard!*) according to the standard procedure described elsewhere.[39]

Ellipsometry measurements of layer thickness were performed using a COMPEL automatic ellipsometer (InOmTech, Inc.). Contact angle was measured with the sessile drop method on a custom-built instrument that combines a microscope and digital camera. Atomic force microscopy (AFM) studies were performed with Dimension-3000 and Multimode microscopes (Digital Instruments) in the tapping mode according to an experimental procedure previously described.[40,41] Surfaces were probed at several random locations using widely varying scan sizes. Molecular models were constructed using Cerius^2 computer modeling program with Dreiding 2.21 force field library on an SGI workstation and Materials Studio 3.0 software using the PCFF force field library for energy minimization and molecular dynamics.

Results and Discussion

Surface Behavior. The rigid, hydrophobic rod core for both molecules is paired with three branched, flexible, hydrophilic PEO chains that possess excellent amphiphilic properties. When placed on water in dilute quantities, these molecules organize into dense monolayers with the hydrophilic PEO branches spread under the water surface, as demonstrated for a number of PEO-containing branched molecules.[42,43] Both molecules displayed stable am-

(24) Whitesides, G. M.; Mathias, J. P.; Seto, C. T. *Science* **1991**, *254*, 1312.
(25) Pao, W.-J.; Zhang, F.; Heiney, P. A.; Mitchell, C.; Cho, W.-D.; Percec, V. *Phys. Rev. E.* **2003**, *67*, 021601−1.
(26) Genson, K. L.; Vaknin, D.; Villacencio, O.; McGrath, D. V.; Tsukruk, V. V. *J. Phys. Chem. B.* **2002**, *106*, 11277.
(27) Mindyuk, O. Y.; Heiney, P. A. *Adv. Mater.* **1999**, *11*, 341.
(28) Ulman, A. *An Introduction to Ultrathin Organic Films*; Academic Press: San Diego, 1991.
(29) Peleshanko, S.; Sidorenko, A.; Larson, K.; Villavicencio, O.; Ornatska, M.; McGrath, D. V.; Tsukruk, V. V. *Thin Solid Films* **2002**, *406*, 233.
(30) Cho B. K.; Jain A.; Gruner S. M.; Wiesner U. *Science,* **2004**, *305*, 5690.
(31) (a) Lee, M.; Kim J.-W.; Peleshanko, S.; Larson, K.; Yoo, Y.-S.; Vaknin, D.; Markutsya, S.; Tsukruk, V. V. *J. Am. Chem. Soc.* **2002**, *124*, 9121. (b) Peleshanko, S.; Jeong, J.; Gunawidjaja, R.; Tsukruk, V. V. *Macromolecules* **2004**, *37*, 6511.
(32) Zubarev, E. R.; Pralle, M. U.; Sone, E. D.; Stupp, S. I. *J. Am. Chem. Soc.* **2001**, *123*, 4105.
(33) Zubarev, E. R.; Stupp, S. I. *J. Am. Chem. Soc.* **2002**, *124*, 5762.
(34) Lecommandoux, S.; Klok, H.; Sayar, M.; Stupp, S. I. *J. Polym. Sci.* **2003**, *41*, 3501.
(35) Yoo, Y.-S.; Choi, J.-H.; Song, J.-H.; Oh, N.-K.; Zin, W.-C.; Park, S.; Chang, T.; Lee, M. *J. Am. Chem. Soc.* **2004**, *126*, 6294.
(36) Lee, M.; Jang, C.-J.; Ryu, J.-H. *J. Am. Chem. Soc.* **2004**, *126*, 8082.
(37) Jayaraman, M.; Frechet, J. M. J. *J. Am. Chem. Soc.* **1998**, *120*, 12996.
(38) Tsukruk, V. V.; Bliznyuk, V. N.; Hazel, J.; Visser, D.; Everson, M. P. *Langmuir* **1996**, *12*, 4840.
(39) Tsukruk, V. V.; Bliznyuk, V. N. *Langmuir* **1998**, *14*, 446.
(40) Tsukruk, V. V. *Rubber Chem. Technol.* **1997**, *70*, 430.
(41) Tsukruk, V. V.; Reneker, D. H. *Polymer* **1995**, *36*, 1791.
(42) Halperin, A.; Tirrell, M.; Lodge, T. P. *Adv. Polym. Sci.* **1992**, *100*, 33.
(43) Mahltig, B.; Jérôme, R.; Stamm, M. *Phys. Chem. Chem. Phys.* **2001**, *3*, 4371.

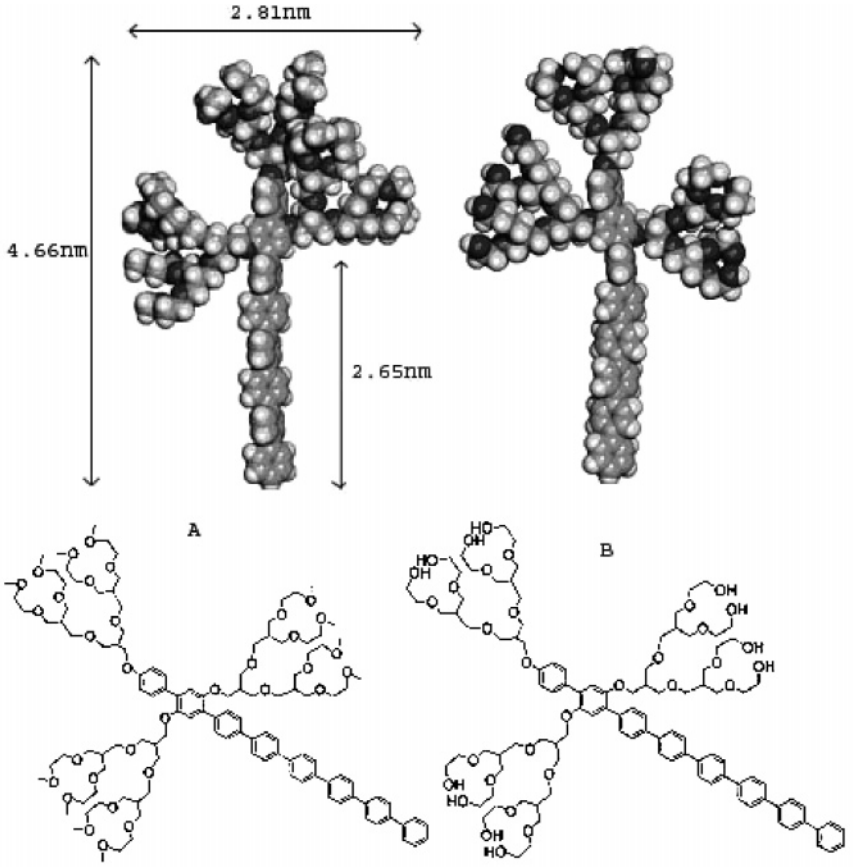

Figure 1. (a) Molecule **1**, methyl-terminated branches and (b) molecule **2**, hydroxyl-terminated branches. Chemical structures are accompanied with molecular models.

Scheme 1. Synthesis of Molecule 2

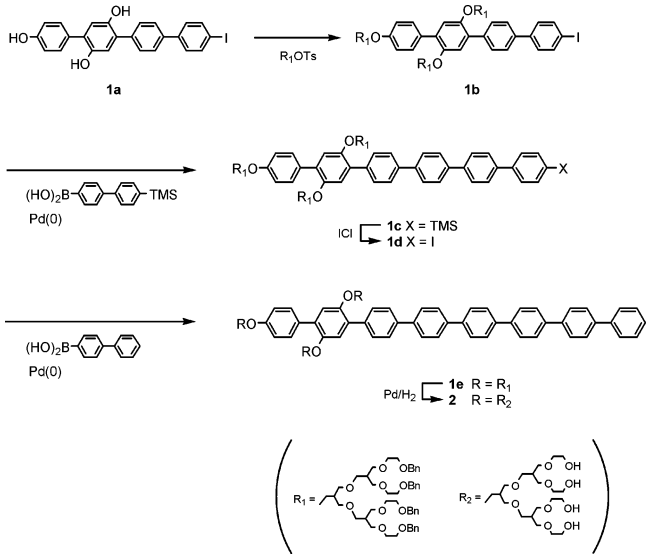

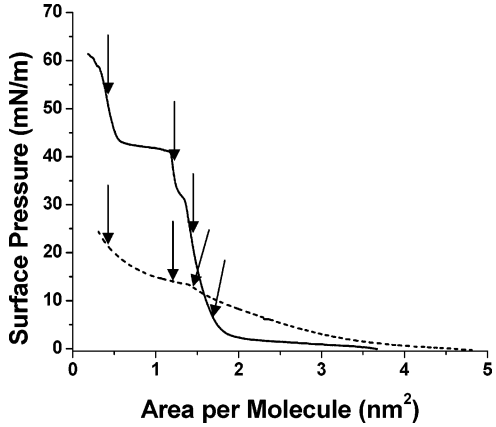

Figure 2. The asymmetric rod−coil molecules form stable Langmuir monolayers at the air−water interface as shown by π−A isotherms for molecule **1** (solid line) and molecule **2** (dashed line) with deposition points indicated by arrows.

phiphilic behavior at the air−water interface. The monolayer compression resulted in steady and reversible increase in surface pressure followed by monolayer collapse at 60 mN/m for molecule **1** and 20 mN/m for molecule **2** (Figure 2). Molecule **1** underwent several phase transitions observed as the multiple shoulders and plateau regions in the pressure versus molecular area (π−A) isotherms. By extrapolating the steepest slope of the isotherm prior to transition states back to a surface pressure of zero, the limiting cross-sectional molecular area in each particular phase can be determined.[28] The initial limiting cross-sectional of molecule **1** (1.68 nm^2) indicated the PEO chains partially submerged into the water subphase. The lower-than-expected cross-sectional area contradicted a face-on orientation of the rod core in favor of a tilted orientation. The observed shoulder at 1.44 nm^2 and the plateau at 1.15 nm^2 indicated the collapse of the initial monolayer due to the organized formation of a bilayer structure. The complete collapse of the monolayer of molecule **1** was observed for molecular areas below 0.5 nm^2. The hydroxyl-terminated molecule lacked the dense packing structure of the first molecule suggested by the larger initial molecular area (2.84 nm^2). A similar shoulder in the π−A isotherm near 1.25 nm^2 was observed for molecule **2**, although the molecule lacked the sharp phase transitions and appeared to collapse at relatively low

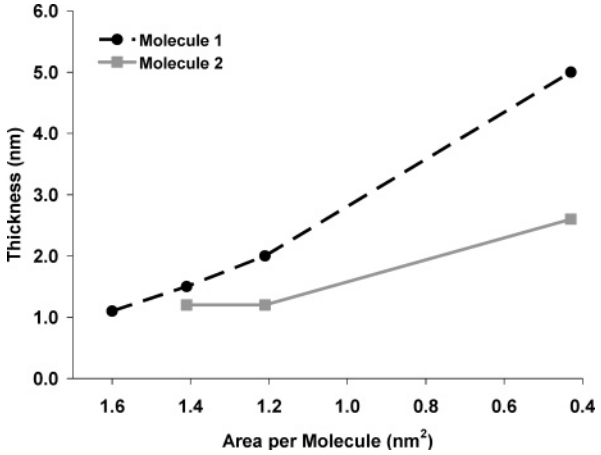

Figure 3. The effective thicknesses of LB monolayers at different densities as determined by ellipsometry.

Table 1. LB Monolayer Properties

sample	area/mol (nm^2)	roughness RMS (nm)	monolayer thickness (nm)	domain height (nm)	contact angle
molecule 1	1.60	0.19 ± 0.02	1.1 ± 0.05	0.0	35 ± 2°
	1.41	0.12 ± 0.02	1.5 ± 0.05	0.0	39 ± 2°
	1.21	0.43 ± 0.02	2.0 ± 0.1	1.9 ± 0.2	41 ± 2°
	0.43	0.75 ± 0.02	5.0 ± 0.1	2.1 ± 0.3	47 ± 2°
molecule 2	1.41	0.19 ± 0.02	1.2 ± 0.05	0.0	53 ± 2°
	1.21	0.21 ± 0.02	1.2 ± 0.05	0.0	55 ± 2°
	0.43	0.58 ± 0.02	2.6 ± 0.1	1.8 ± 0.2	62 ± 2°

surface pressures. Both molecules were deposited at multiple cross-sectional areas of interest to elucidate the nature of intra-monolayer reorganization (see arrows in Figure 2).

The low effective thickness of monolayers deposited at cross-sectional areas above 1.0 nm^2 further suggested the rigid rod core packed loosely above the spread PEO chains (Figure 3, Table 1). The measured thickness (1.1−1.5 nm for molecule **1**, 1.2 nm for molecule **2**) for the less-dense monolayers supported the idea of the rigid cores supported by the spread PEO branches at the air−water interface. Both molecules followed the same general trend expected for PEO-containing branched molecules,[44] with lower thickness indicating greater segregation of the hydroxyl-terminated PEO chains in molecule **2**. Reduction of the molecular area below the observed phase transitions (1.2 nm^2 for both molecules) compelled a 2-fold increase in monolayer thickness (Table 1). Further compression of molecule **1** below 0.5 nm^2 per molecule compelled the largest increase in effective thickness attributable to the multilayer formation upon complete monolayer collapse.

The surface composition of the deposited monolayers was revealed by analyzing the water contact angle. The deposited monolayers for both molecules exhibited low to moderate hydrophobic character (contact angle in the range of 35−62°), indicating a mixed surface composition (a contact angle of 80−120° is expected for surface composed of phenyl rings). Contact angle measurements revealed increasing hydrophobicity for denser monolayers associated with greater exposure of hydrophobic fragments (Table 1). The contact angle measurements for molecule **2** indicated a more hydrophobic surface that can be associated with larger submerging of hydroxyl-terminated PEO chains resulting in less exposure at the air-solid interface. As a result, the interactions of the hydrophilic groups are better shielded, resulting in an increase of the effective contact angle.

(44) Genson, K. L.; Huffman, J.; Teng, J.; Zubarev, E. R.; Vaknin, D.; Tsukruk, V. V. *Langmuir* **2004**, *20,* 9044.

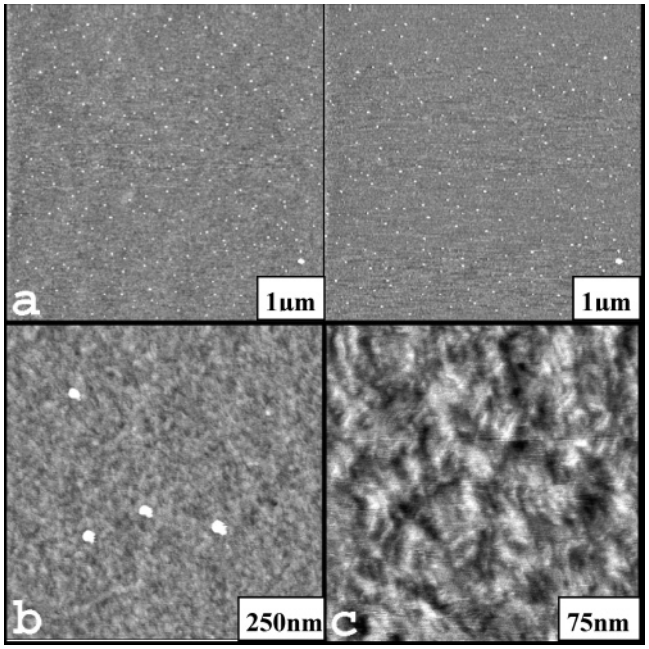

Figure 4. AFM images of LB monolayer from molecule **1** deposited at 1.60 nm^2. (a) 5 × 5 μm^2 scan, topography (left image) and phase (right image). Height z range = 5 nm, phase z range = 20°. (b) 1 × 1 μm^2 AFM topography scan. Height z range = 5 nm. (c) 300 × 300 nm topography. Height z range = 2 nm.

Table 2. Calculated Structural Parameters vs Observed Values for Molecule 1 Structures

parameter	calculated	observed
ring diameter	11.5 nm	10.8 ± 0.95 nm
ribbon bilayer (width)	6.8 nm/period	15−35 nm
ribbon bilayer (height)	1.9 nm	1.9 ± 0.2 nm

Surface Morphology. Molecule **1** formed uniform monolayers for thin films deposited at the lowest surface area per molecule (1.60 nm^2), as shown in Figure 4. High-resolution AFM exhibited a disordered, fingerlike lamellae structure arranged in groups of two or more rows (Figure 4c). Cross-sectional analysis revealed the lamellae width was 4−8 nm, with 3−5 nm spacing, and were approximately 30 nm long and 0.5 nm high observed the surrounding monolayer. Similar surface morphology was observed for LB monolayers deposited at lower cross-sectional areas (1.41 nm^2) with the more-pronounced lamellar structures. The slight reduction of molecular area resulted in a reduction of RMS roughness in addition to a small increase in effective thickness, suggesting the monolayer experienced an increased in uniformity and thickness (Table 1).

At a lower cross-sectional area of 1.21 nm^2 (above the first shoulder on the surface-pressure isotherm, Figure 2), significant changes of surface morphology accompanied by a significant increase in thickness were observed (Table 2, Figure 5). At this molecular area, the formation of anizodiametric domains occurred. Long, thin domains were readily seen, with occasional cases of neighboring domains aggregating together and forming a doubly wide structure. The long, thin domains can be seen to be aligned in the horizontal direction, which is perpendicular to the dipping direction, indicating an important role of the vertical lifting in domain orientation, as well as high mobility. Occasionally, the domains terminated in much wider, irregular structures, as seen in Figure 5b. These secondary surface structures are comprised of flat, irregular-shaped domains of several hundred nanometers.

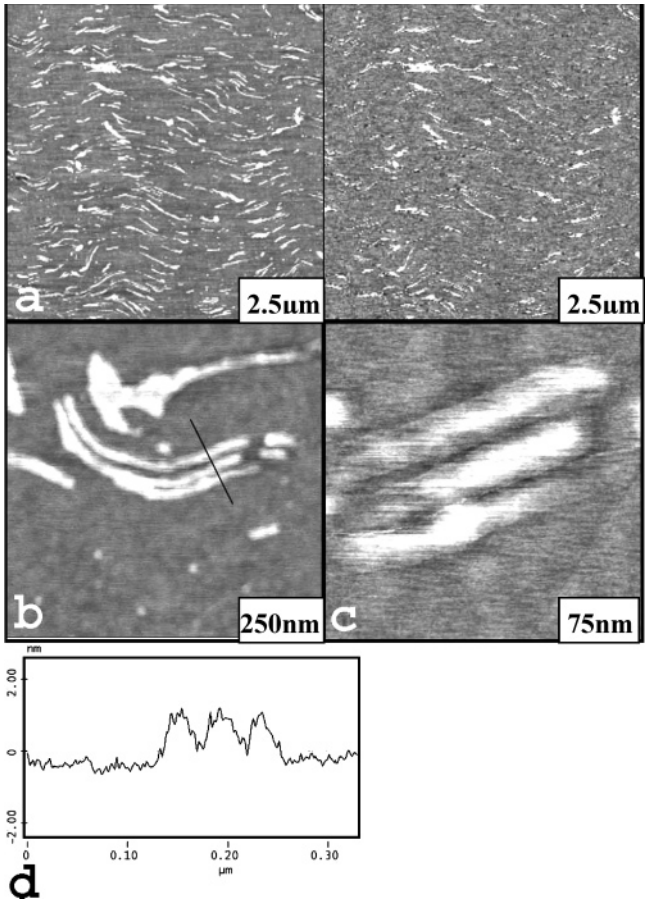

Figure 5. AFM images of LB monolayer from molecule **1** deposited at 1.21 nm^2. (a) 10 × 10 μm^2 scan, topography (left), z range 10 nm and phase (right), z range 10°. (b) 1 × 1 μm^2 scan (topography), z range 5 nm. (c) 300 × 300 nm scan (topography), z range 5 nm. (d) Line cross-section (line in (b)) shows domain height of 1.3−1.5 nm and the average thickness of 33 nm.

These domains, with a thickness of 3 nm, represented secondary, topmost layers which started forming at high lateral compression of the underlying monolayer as an initial stage of the bilayer formation in the precollapsed state.[28] Cross sections of the AFM images revealed the height of the ribbonlike domains of 1.5 nm (Figure 5d). The true width of the thin domains ranges from 15 to 35 nm, accounting for tip dilation.

High-resolution AFM imaging of larger, flat, and thicker bilayer domains of up to several hundred nanometers across revealed the presence of very fine, ring-shaped surface nanostructures randomly packed within the topmost surface of the outer layer (Figure 6a). The ring diameter determined from the distance between their rims unaffected by the AFM tip dilation was very uniform for all rings observed (Figure 6b). These ring structures were analyzed by multiple cross-sections and found to have overall external diameters of 9−12 nm with an interior opening of smaller than 8 nm (see cross-section in Figure 6) (Table 2).

Replacement of the hydrophobic terminal groups in molecule **1** with hydroxyl groups in molecule **2** resulted in complete disappearance of the surface nanostructures observed for molecule **1**. The comprehensive study of molecule **2** revealed only uniform surface topography without any signs of characteristic surface micellar structures. Obviously, for this molecule with an additional 12 hydroxyl terminal groups, the amphiphilic balance is shifted toward highly hydrophilic branched PEO. This resulted in a much less stable monolayer due to the tendency of the molecules to sink into the subphase at higher lateral compression without forming organized 2D structures.

Models of Molecular Packing in Monolayers. Here, we consider possible molecular packing for the treelike molecule **1** observed in the condensed state of the LB monolayer. First, it is clear that the relatively low thickness of 1−1.5 nm for the monolayer along with the mixed surface presence of hydrophobic and hydrophilic fragments effectively excludes a model of a densely packed monolayer featuring vertical orientation of the rodlike fragments. Thus, a major element of any molecular packing should be a flat orientation of the molecules with hydrophilic branches spread beneath the hydrophobic rod fragments (Figure 7).

Second, due to the large cross-sectional mismatch between the hydrophobic rods and hydrophilic branches, spherical or cylindrical aggregates should be preferably formed in the solution as was already revealed.[36] The two-dimensional analogue of these highly curved spherical aggregates are circular structures which can fill out on a planar interface (Figure 7). Steric interactions should naturally place the rodlike fragments in the interior which will be stabilized by strong hydrophobic interactions between polyphenylene chains, while the bulkier hydrophilic branches should make up the outer edge of the ring. Finally, considering significant steric mismatch, ribbonlike surface structure can be formed from these molecules only under the condition of significant lateral compression. Under this compression, the bulkier hydrophilic branches can be displaced from the interface and submerged while rodlike fragments should interdigitate to compensate for remaining cross-sectional mismatch (Figure 7).

The models of possible molecular packings discussed above describe fairly well the two surface structures, ribbonlike and circular, observed for molecule **1** at high surface pressures. The lateral dimension of the model of the circular aggregate proposed is evaluated to be about 11 nm, which is very close to AFM data on lateral dimensions (Figures 7, Table 2). The thickness of this molecular structure below 2 nm fits to experimental results on the second layer thickness as well. The planar, layered structure suggested as an alternative packing model can be assigned to the thin, ribbonlike surface structures (Figure 5). The effective width of the interdigitated packing suggested in this model of about 7 nm is close to the effective width of poorly visible lamellar structures observed in a loosely packed monolayer, indicating initial stages of its formation under low lateral compression. At much higher lateral compression, the ribbonlike structures of 15−35 nm packed in correlated manner are several times wider than the width of an individual bilayer (Figure 5, Table 2). This indicates the multilayered internal structure of ribbons composed of several (from 2 to 5) correlated planar layers.

The formation of ribbonlike structures within the monolayer at lateral compressions close to collapse is consistent with expectations for conditions needed for this type of packing. We suggest that initial rupture of some monolayer areas on the verge of the monolayer collapse followed by the formation of the bilayer surface domains releases the lateral pressure and creates conditions for assembling circular planar structures within the topmost layers. The topmost molecules within the bilayer domains are situated on top of an underlying mixed monolayer that is more favorable for circular packing of these asymmetric molecules by preventing direct interactions with the solid surface. Confinement of the bilayer domains at the interface restricted three-dimensinal micellar

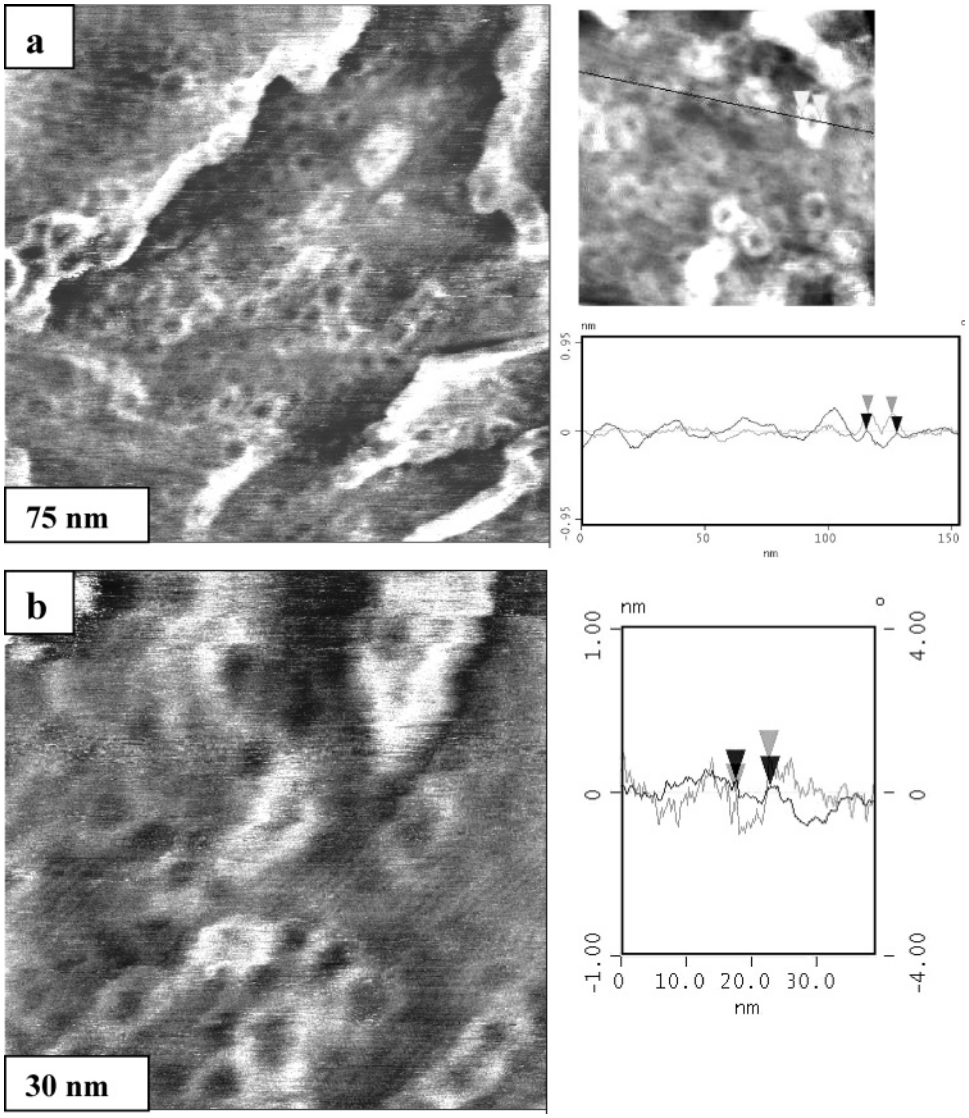

Figure 6. High-resolution phase images of LB monolayer from molecule **1** at molecular area 1.21 nm^2 (a, b) and representative cross-sections of a ring structure; gray line is phase and black line is topography with markers showing rim-to-rim distance.

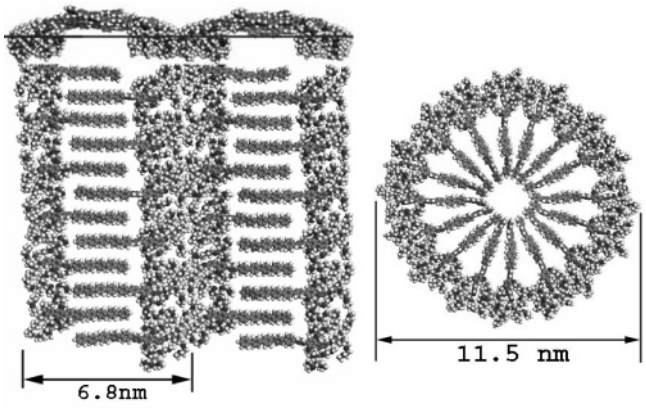

Figure 7. Molecular model of molecule **1** packing showing interdigitated layering (left) and a circular planar structure (right).

formation and initiated two-dimensional circular micelles. This is in contrast to the preferred three-dimensional spherical aggregates observed in solution for similar molecules when interfacial interactions do not contribute.[35,36] Similar to the spherical micelle formation in dilute solutions, the circular micelles were preferentially formed when the lateral compression was released. However, the location of the domains at the air−water interface confined the micelles to a two-dimensional shape versus the three-dimensional spheres formed in solutions. In addition, we believe that the presence of 12 hydrophobic terminal groups in hydrophilic PEO branches is a critical factor in the formation of these surface structures. Their presence stabilizes the formation of organized surface structures, not allowing the PEO chains to completely submerge in the water subphase during lateral compression, as usually observed for noncapped PEO chains in branched molecules.[45,46]

Although the structural reorganizations within the monolayers observed here for treelike molecule **1** resemble those observed for other amphiphilic rod−coil and star molecules reported recently,[8,44] the branching of hydrophilic fragments makes significant difference in their surface behavior. In fact, linear rod−coil molecules exhibited transformation from rectangular packing of molecular clusters at low surface pressure to well-ordered layering at high surface pressure caused by the submer-

(45) Cox, J. K.; Yu, K.; Eisenberg, A.; Lennox, R. B. *Phys. Chem. Chem. Phys*. **1999**, *1*, 4417.
(46) Richards, R. W.; Rochford; B. R., Webster, J. R. P. *Polymer* **1997**, *38* 1169.

gence of hydrophilic end blocks in the water subphase. This is unlike the dendritic−rod molecules studied here, which showed interdigitated layering caused by their asymmetric character already at low surface pressure and circular micellar structures in the precollapsed state. In their two-dimensional state within the monolayers, these treelike molecules adopt the wedged shape which is favorable for the assembling of a variety of highly curved organized structures already found in the bulk state for multibranched molecules.[47] We suggest that the confinement of the compressed monolayers imposed by the planar interface combined with lateral pressure enforced the formation of the interdigitated layering instead of the highly curved cylindrical or spherical micellar structures favorable for these molecules in solution. Partial submergence of the hydrophilic branches in the water subphase combined with this interdigitated layering of the rigid fragments provided an appropriate combination for dense intra-monolayer packing of these highly asymmetrical molecules at the planar interfaces. To the best of our knowledge, such circular surface structures within planar monolayers have been never observed before.

Acknowledgment. Funding from the National Science Foundation, Grant No. DMR-0308982, and support from Creative Research Initiative Program of the Korean Ministry of Science and Technology are gratefully acknowledged. We thank Sergey Peleshanko for technical assistance.

Supporting Information Available: Synthetic procedures. This material is available free of charge via the Internet at http://pubs.acs.org.

LA0504107

(47) (a) Percec, V.; Glodde, M.; Johansson, G.; Balagurusamy, V. S. K.; Heiney, P. A. *Angew. Chem., Int. Ed.* **2003**, *42*, 4338. (b) Jung, H. T.; Kim, S. O.; Ko, Y. K.; Yoon, D. K.; Hudson, S. D.; Percec, V.; Holerca, M. N.; Cho, W.-D.; Mosier, P. E. *Macromolecules* **2002**, *35*, 3717. (c) Pao, W.-J.; Stetzer, M. R.; Heiney, P. A.; Cho, W.-D.; Percec, V. *J. Phys. Chem. B* **2001**, *105*, 2170. (d) Percec, V.; Cho, W.-D.; Ungar, G. *J. Am. Chem. Soc.* **2000**, *122*, 10273. (d) Yeardley, D. J. P.; Ungar, G.; Percec, V.; Holerca, M. N.; Johansson, G. *J. Am. Chem. Soc.* **2000**, *122*, 1684. (e) Hudson, S. D.; Jung, H.-T.; Percec, V.; Cho, W.-D.; Johansson, G.; Ungar, G.; Balagurusamy, V. S. K. *Science* **1997**, *278*, 449. (f) Percec, V.; Ahn, C.-H.; Ungar, G.; Yeardley, D. J. P.; Moller, M.; Sheiko, S. S. *Nature* **1998**, *391*, 161.